Technical report; TR-196

KNMI

Environmental and Climatic Consequences of Aviation

Final report of the KNMI contributions to the AERO-project

Wiel Wauben, Peter van Velthoven and Hennie Kelder

De Bilt, 1997

Technical report = technisch rapport; TR-196

De Bilt, 1997

P.O. Box 201
3730 AE De Bilt
Wilhelminalaan 10
Telefoon 030-220 69 11
telefax 030-221 04 07

Authors: Wiel Wauben
Peter van Velthoven and
Hennie Kelder

UDC: 551.583.1
551.521.32
656.7

ISSN: 0169-1708

ISBN: 90-369-2116-3

● ● ● ●

Environmental and Climatic Consequences of Aviation

Final report of the KNMI contributions to the AERO-project

Wiel Wauben, Peter van Velthoven and Hennie Kelder

KNMI, PO Box 201, 3730 AE De Bilt, The Netherlands

January, 1997

1. Introduction

The RLD (Dutch Civil Aviation Authorities) has started a policy analysis in order to find the best strategy to reduce the impacts of air traffic on the atmosphere taking into account the environmental benefits, as well as the economic impacts for the aviation industry. This is done in the AERO-project (Aviation Emissions and Evaluation of Reduction Options). The project is executed by the KNMI (Royal Netherlands Meteorological Institute), MVA-Consultancy, the NLR (National Aerospace Laboratory), Resource Analysis, and the RLD. A description of the project is given by Pulles *et al.* (1995). The AERO-project will lead to the construction of AIMS (Aviation Immission Modelling System), which is a software shell integrating all AERO modules. A user interface will allow for the specification of scenarios, different policy measures, as well as various other assumptions. This AIMS system will be used in order to asses the environmental and economic impacts of air traffic policies.

The KNMI investigates the environmental and climatic consequences of aircraft emissions and therefore participates in the construction of the APDI and ENVI modules of AIMS. APDI (Atmospheric Processes and Dispersion model) determines the three-dimensional concentrations for all relevant substances and ENVI (direct and indirect Environmental Impact model) assesses impacts on global warming and changes in ultraviolet radiation at the ground. These modules are part of the integrated AIMS model so that the advanced chemistry transport model and radiative transfer models which are used to calculate the above mentioned impacts cannot be used due to computer restrictions. Therefore parametrizations of these processes had to be developed. In this report the KNMI contributions to the AERO-project are described.

2. APDI: Atmospheric processes and dispersion calculations

In the first phase of the AERO-project the global three-dimensional chemistry transport model of the KNMI (CTMK) has been used to study changes in atmospheric NO_x (=NO+NO_2) and ozone concentrations due to aircraft emissions (cf. Wauben *et al.*, 1995a). The CTMK model has been used for previous studies of the impact of aircraft emissions on the atmosphere (e.g. Wauben *et al.*, 1994; AERONOX, 1995; Wauben *et al.*, 1997a) and the results were in agreement with those obtained with other models. Furthermore, CTMK has been validated versus observations (Emmons *et al.*, 1997; Wauben *et al.*, 1997b; Wauben *et al.*, 1997d).

The complex CTMK model is presently not suitable for use in AIMS because of computer performance limitations. Therefore parametrizations had to be constructed which give the three-dimensional concentrations for all relevant atmospheric constituents. Atmospheric constituents like CO_2 with long chemical lifetimes accumulate in the atmosphere. These species can be homogeneously distributed in the atmosphere taking into account the past emissions of the species. Constituents like NO_x and ozone with shorter lifetimes are more difficult to parametrize since both chemistry and transport need to be considered. For these tracers CTMK is used to construct repro functions. The repro function that is constructed for CTMK is a transfer matrix that gives the change in the three-dimensional concentration of a tracer when emissions occurs in an individual grid cell. The distribution of trace gases is obtained as a difference with an actual distribution pre-calculated with CTMK for a certain emission scenario, by computing the changes induced by the differences in the emissions with the transfer matrix. Due to the non-linearity of the system, the use of the transfer matrix is restricted to a certain range in emissions. In order to enhance this range the three-dimensional distribution of trace gases pre-calculated for several different scenarios serve as situations to which the repro function can be applied. Alternatively, an interpolation between these pre-calculated trace gas distributions can be considered. In order to construct a transfer matrix many runs with the CTMK model are required. In the second phase of the AERO-project (cf.

Wauben *et al.*, 1995b) test calculations for the development of the transfer matrices were performed. These calculations also served to select an optimal method for computing the results required to construct the repro functions.

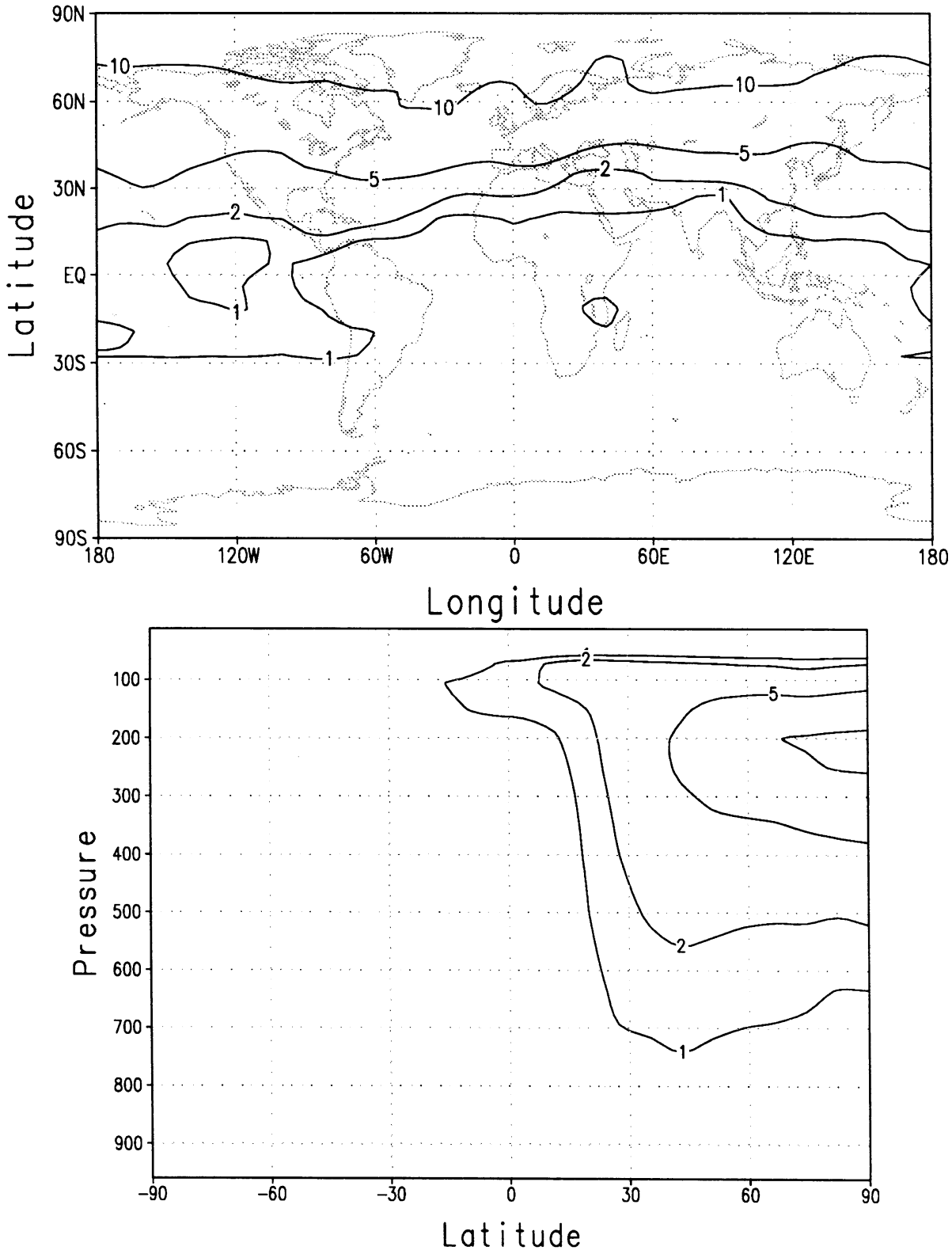

Figure 1. The ozone perturbation (in ppbv) caused by aircraft NO_x emissions for July. Shown are the geographical distribution at 200 hPa (top) and the zonal mean distribution (bottom).

In addition, several scenarios have been calculated with CTMK. An extensive description of the global three-dimensional distribution of nitrogen oxides and ozone and the perturbation caused by aviation resulting from 1990, 2003 and 2015 emission scenarios is given in Wauben *et al.* (1995b). Note that the emissions used for these calculations were not generated by the AERO modules FLEM and OATI. Such runs are essential in order to fix some situations between which the repro function can be used. This reduces the range over which the repro functions have to be applied, and thus reduces errors introduced by these functions. In addition, the pre-calculated CTMK results are used for illustrating purposes. Therefore, new calculations with CTMK will be performed using emissions generated by AIMS as soon as these data become available. In this report, results using the ANCAT aircraft emission inventory, will be presented to illustrate the modules. Figure 1 shows the geographical distribution at 200 hPa and the zonal mean distribution of the aircraft induced changes of ozone for July calculated with CTMK. The largest changes are found around cruise altitudes on the northern hemisphere.

2.1 APDI parametrization for long lived species

The distribution of gases with relatively long residence times in the atmosphere is determined according to a procedure similar to the one described by Fortuin *et al.* (1995), i.e., by distributing these species homogeneously throughout the atmosphere and using a constant atmospheric residence time. Assume that starting at time t_0 (in years) the CO_2 emisisons E (in Tg/yr) increases linearly in time t according to the relation

$$E(t) = E_0 + \alpha(t - t_0), \tag{1}$$

where α (in Tg/yr^2) is the increase in emissions with magnitude E_0 at time t_0. The time evolution of the total mass loading $M(t)$ for $t > t_0$ of a long lived gas is given by

$$\frac{dM(t)}{dt} = -\frac{M(t)}{\tau} + E(t), \tag{2}$$

with τ (in years) the residence time of the gas in the atmosphere. The first term on the right-hand side of Eq. (1) describes the decrease in mass loading of the gas whereas the second term gives the increase due to emissions. The solution of Eq. (2) considering a boundary condition $M(t_0)$ for the mass loading at time $t = t_0$ is

$$M(t) = \tau E(t) + \alpha\tau^2\{\exp[-(t - t_0)/\tau] - 1\} + \{M(t_0) - E_0\tau\}\exp[-(t - t_0)/\tau]. \tag{3}$$

Fortuin *et al.* (1995), based on recordings of aircraft fuel burn data and assuming a CO_2 emission index is 3.15 kg per kg fuel emitted, estimated an increase for the CO_2 emitted by aviation of α= 3.7 Tg/yr^2 starting with $M(t_0)$=0 at t_0=1943. A mass loading of 11073 Tg CO_2 due to aviation up to 1990 can be obtained from Eq. (3) using an atmospheric residence time for CO_2 of 100 year. Next, the mass loading is distributed equally over the entire atmosphere and converted to volume mixing ratios by using

$$\Delta CO_2 = M(t)/M_{atm} \times m_{air}/m_{CO_2} \tag{4}$$

with the total mass of the atmosphere $M_{atm} = 5.10^9$ Tg, the molecular air mass m_{air} =28.94 and the molecular CO_2 mass m_{CO2} =44.01. For 1990 this gives an increase of atmospheric CO_2 due to aircraft ΔCO_2 of 1.43 ppmv at every geographical location, altitude and season. Note that the background CO_2 mixing ratio was 352 ppmv in 1990 which increased by about 1.5 ppmv/yr (IPCC, 1995).

2.2 APDI parametrization for short lived species

The global three-dimensional distribution of gases with relatively short residence times in the atmosphere is more difficult to calculate because of the strong interaction between transport and chemistry. For the construction of a transfer matrix calculations were performed with emissions in a single grid cell of CTMK. The results of these calculations are reported by Wauben *et al.* (1995b). Figure 2 illustrates the latitude and altitude dependence of the global change in NO_x and O_3 when the same amount of 10 kton NO_2 is introduced in the form of NO_x in each grid cell (0-90°N and 1000-175 hPa), separately. Figure 2 shows that the resulting ozone perturbation increases with altitude and from the equator towards the pole.

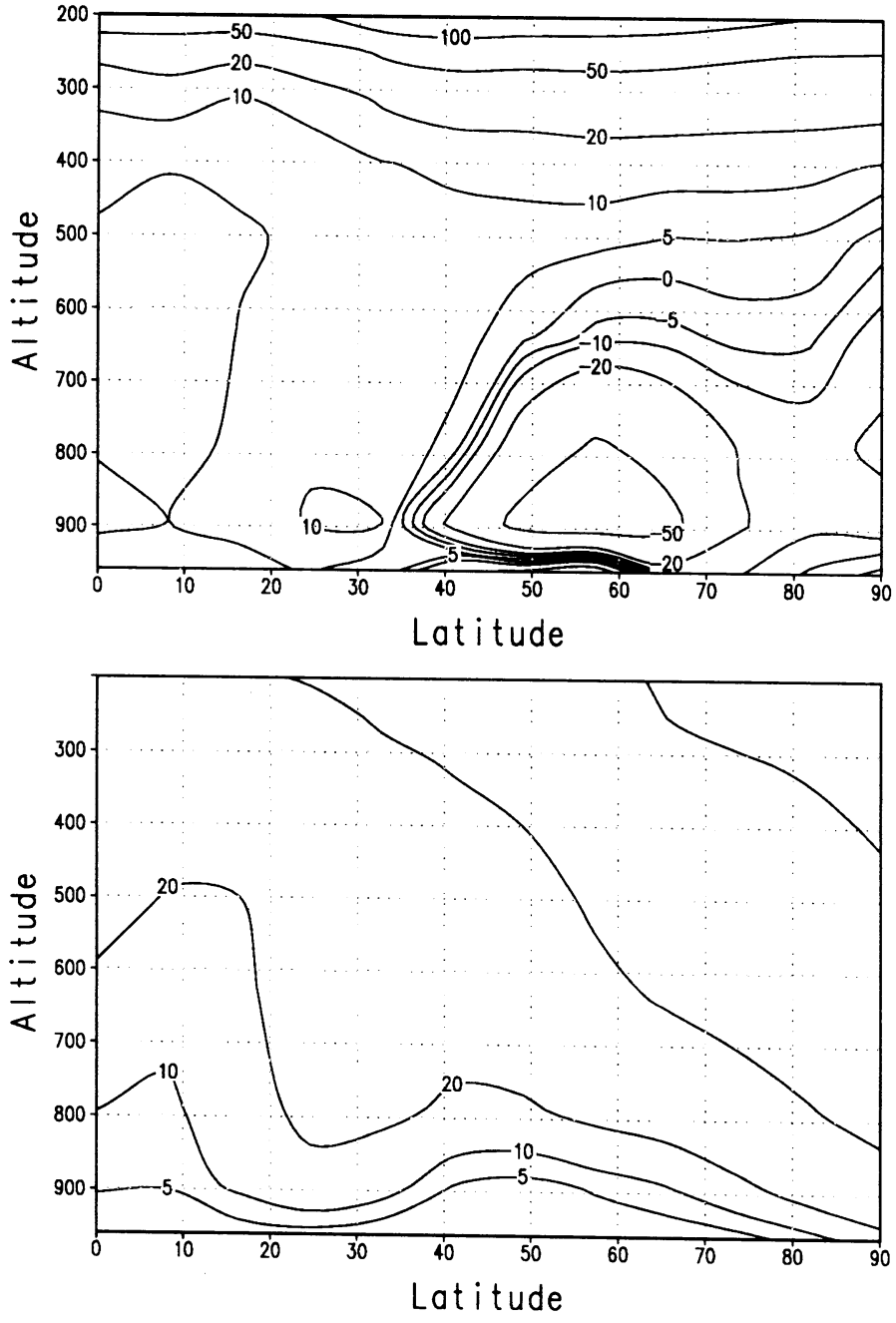

Figure 2. The global change in NO_x (top: in ton N) and ozone (bottom: in kton) as a function of the latitude and altitude of a NO_x perturbation of identical magnitude.

3. ENVI: Calculations for direct and indirect environmental impact

Changes in atmospheric composition due to aircraft emissions are calculated in the APDI module. The environmental impacts resulting from these changes determine whether action should be undertaken to reduce the emissions that caused these impacts. The contribution of aircraft emissions to two environmental impacts have been investigated at KNMI within the framework of the AERO-project:

(i) Changes in atmospheric constituents may alter the radiation budget of the Earth. The resulting climate effects are studied by using the concept of radiative forcing, i.e. the net change in radiation at the tropopause.

(ii) Changes in ozone influence the amount of damaging ultraviolet radiation that reaches the surface.

3.1 ENVI parametrization for radiative forcing

Aircraft emissions introduce many pollutants in the atmosphere that contribute directly or indirectly to radiative forcing. First estimates for the radiative forcing of different components were given by Fortuin *et al.* (1995). These results were obtained by using literature estimates for the increase of the various components due to aircraft emissions and pertain to northern midlatitudes. In the AERO-project the ozone perturbation as calculated by CTMK is used in KRCM (KNMI Radiative Convective Model) in combination with the actual temperature and humidity profiles (see Wauben *et al.*, 1995b) to obtain the resulting radiative forcing. The altitude of the tropopause, where the radiative forcing is specified, is calculated from the temperature profile. The surface albedo is taken from the global data set of Matthews (1983). Figure 3 shows the radiative forcing due to the ozone changes from aviation for July. The maximum radiative forcing is located at northern mid-latitudes and its magnitude agrees with the estimates given by Fortuin *et al.* (1995). Note that the maxima do not occur at the location of the maximum ozone perturbation, but are shifted to regions with higher radiation levels (i.e. higher solar elevation or higher surface temperature) since a perturbation gives a larger change in radiation if more radiation is present. In the case of ozone, especially the long wave radiation contributes to the radiative forcing.

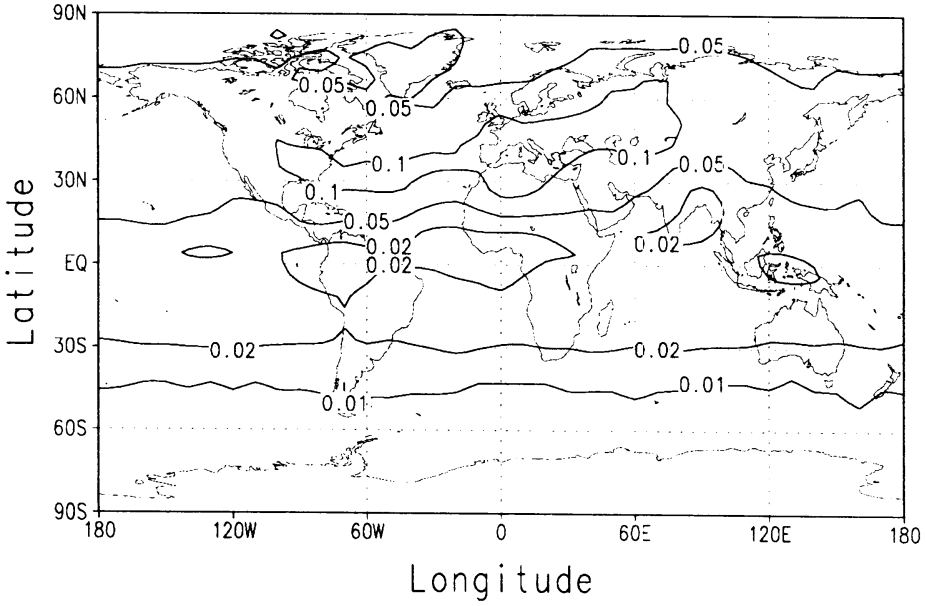

Figure 3. Radiative forcing (in W/m^2) due to ozone changes from air traffic for July.

The calculation of the radiative forcing in ENVI is performed using a global set of sensitivity curves, each of which gives the radiative forcing as a function of the changes in ozone at every vertical level (cf. Fortuin *et al.*, 1995; Wauben *et al.*, 1997c). The sensitivity curves were constructed by perturbing the background ozone distribution in each layer with 1 DU. The spatial dependence of the radiative forcing caused by a uniform ozone increase of 1 DU in each layer is illustrated in Fig. 4, which shows (a) the geographical cross-section of the induced radiative forcing at 200 hPa and (b) the latitude-altitude cross-section at 0°W. Figure 4a clearly illustrates the latitudinal dependence of the sensitivity with high values in the tropics and low values in the polar regions. The longitudinal dependence can be observed as a higher sensitivity over the continents than over the oceans in the summer hemisphere, which is a result of the higher surface temperatures over the continents leading to a larger radiative impact. The vertical dependence of the sensitivity of radiative forcing to ozone changes is presented in Fig. 4b. Maximum sensitivity is obtained at the tropopause which decreases from the equator to the poles. The effect of the high temperatures in the Sahara are also visible in Fig. 2b. Negative sensitivity, i.e., a decrease in net downward irradiance at the tropopause due to an ozone increase, is found in almost the entire illuminated stratosphere and in the polar lower troposphere during the polar night.

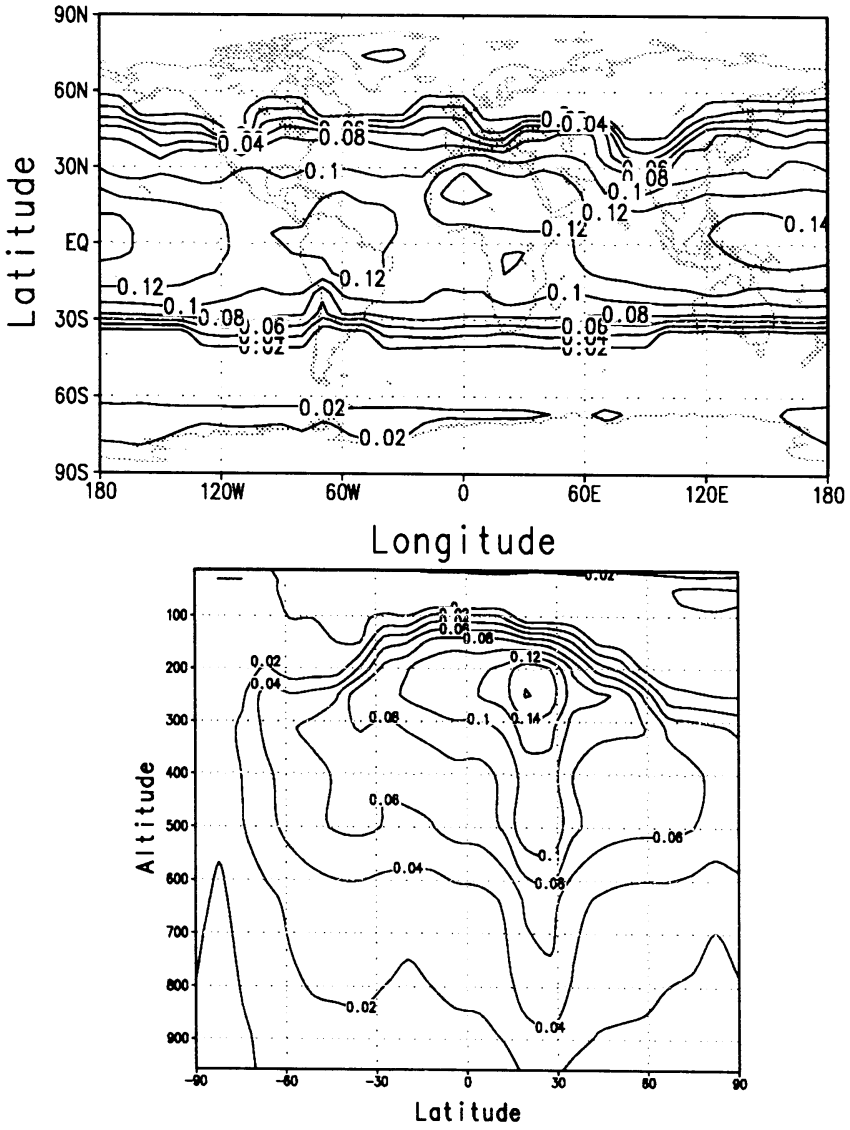

Figure 4. Cross-sections of the sensitivity of radiative forcing (in W/m^2) due to a 1 DU ozone increase in each grid cell for July at 200 hPa (top) and at 0°W (bottom).

The geographical distribution of radiative forcing RF (in W/m^2) of an aircraft induced perturbation of the ozone field can be calculated as follows. First calculate the ozone change $\Delta O_3(k)$ (in DU) for each layer k above a grid cell of CTMK denoted by longitude cell i and latitude cell j. Next calculate the radiative forcing according to

$$RF(i,j)=\Sigma_k \Delta O_3(k)\, SC(i,j,k) \tag{5}$$

where $SC(i,j,k)$ is the sensitivity curve as a function of the layer of CTMK which depends on the geographical position (i,j) and the season (January or July).

The radiative forcing due to changes in CO_2 has been parameterized in a similar way. However, because CO_2 is distributed homogeneously in the atmosphere, the forcing resulting from a uniform change with altitude is calculated. Thus, the sensitivity of radiative forcing to CO_2 changes depends only on longitude and latitude, and not on altitude.

The radiative forcing is the change in net downward radiation at the tropopause. When this forcing has the same magnitude in summer and winter, but with opposite signs, then it still has a climate effect. Therefore averaging/combining the January and July values in an annual value does not make much sense. The extreme values, which are generally reached in January and July are more fundamental.

3.2 ENVI parametrization of damaging ultraviolet radiation

Many factors control the amount of UV radiation that reaches the surface. A complex radiative transfer model is needed in order to account for all these factors such as the solar elevation, the ozone column, the aerosol (small particles) loading of the atmosphere, clouds, the surface pressure and the surface reflectance. Such a model requires too much computer time and besides, the characteristics of aerosol and the effects of clouds are not well known at present. Therefore an empirical relation is used in ENVI that gives the amount of damaging UV radiation reaching the surface in terms of an analytical expression involving the ozone column Ω (in DU) and the solar elevation γ (in degrees). The relation reads

$$DUV = \sin\gamma \exp[A+B\Omega/\sin\gamma+C/\sin\gamma+D(\Omega/\sin\gamma)^2+E/(\sin\gamma)^2] \tag{6}$$

where the constants A=7.093, B=–3.927 10^{-3}, C=–0.636, D=1.525 10^{-6} and E=0.1183 have been determined from a fit to actual clear sky damaging UV data (cf. Kuik and Kelder, 1994). The above mentioned empirical relation is only valid for solar elevations larger than 21 degrees. For lower solar elevations the relation

$$DUV = 0.7578–0.2241\gamma+0.0472\gamma^2 \tag{7}$$

is used. Note that the relations are discontinuous at a solar elevation of 21 degrees. The relation takes the dependence of the damaging UV on the incident solar irradiance, solar elevation, ozone and aerosol up to some degree into account. A correction for the surface elevation is made by calculating first the elevation h (in km) from the surface pressure P_s (in hPa) using a scale height of 8.2 km

$$h = -8.2 \log(P_s/1013.25), \tag{8}$$

and then increasing the damaging UV by 15% per altitude step of 1 km, i.e.

$$DUV = (1.+0.15h)\, DUV. \tag{9}$$

The influence of the surface albedo is neglected. The presence of clouds is not taken into account, but since its effect may lead to an decrease of damaging UV due to screening of the sun as well as an increase of damaging UV when no clouds are blocking the sun and reflection at cloud edges enhances the irradiance at the surface, the averaged damaging UV values do

only decrease significantly if the sky is almost completely covered with clouds. The relation for damaging UV is illustrated in Fig. 5 which gives the damaging UV irradiance reaching the surface as a function of local time. The effect of variations in the ozone column is also indicated. The observed damaging UV curve is found to agree reasonably well with the corresponding empirical curve.

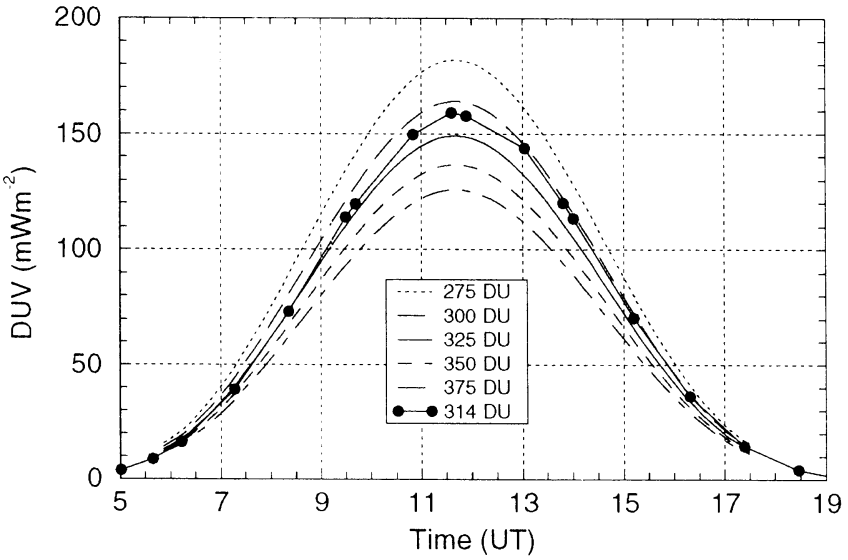

Figure 5. Computed and measured diurnal variation of damaging UV for various total ozone columns.

Damaging UV (in W/m^2) is obtained by multiplying the spectral UV radiation with the sensitivity of the human skin to sun burn and integrated over wavelength. The damaging UV has been calculated according to the above equations using actual ozone columns observed daily by TOMS for 1990. For every horizontal grid box of CTMK the TOMS ozone columns are considered in combination with the actual solar elevation at all 1 hour intervals. Monthly effective UV values (in J/m^2), i.e., damaging UV integrated over time, have been calculated from these damaging UV values for each horizontal grid box. It was found that the longitudinal dependence of the monthly effective UV values is small (when the effect of the surface elevation is neglected), so that only its latitudinal and seasonal dependence needs to be considered. Furthermore, it was found that calculating the damaging UV values for the 15th of each month by using zonal mean climatological values for the ozone columns and calculating the monthly effective UV by integrating the damaging UV over these days multiplied with the number of days in each month gives about the same monthly effective UV values as those obtained by using the daily TOMS data. The second approach which uses the zonal mean monthly mean ozone data is therefore applied here. The calculated monthly effective UV is given in Fig. 6 for each latitude of the CTMK grid used for the AERO calculations.

Next the change in effective UV resulting from a change in the ozone column is considered. For that purpose the monthly effective UV is calculated from the zonal and monthly mean ozone columns, which are for this purpose changed by a fixed value. The difference in the monthly effective UV values obtained with the zonal and monthly mean ozone columns and those obtained with the zonal and monthly mean ozone columns increased by 10 DU divided by the change in the ozone column, i.e. (EUV(Ω+10)-EUV(Ω))/10, is also shown in Fig. 6. The effective UV does not vary linearly with the ozone column. Therefore, this particular sensitivity of effective UV to the ozone column can be applied only in a restricted range of ozone column values. For each longitude and latitude denoted by cell i and j, respectively, the change in the ozone column, $\Delta\Omega(i,j)$, in both January and July can be calculated with the output of APDI. For this purpose the change in the ozone mass mixing ratio

for each layer k must be multiplied with the total mass of the grid box whereafter the ozone mass changes are summed over all layers and converted into Dobson units. Next the effective UV and its change can be calculated using

$$EUV(i,j) = EUV(j) + \Delta\Omega(i,j)\,\Delta EUV(j) \tag{10}$$

Here $EUV(j)$ is the monthly effective UV as a function of latitude calculated from the empirical relation for the damaging UV by using the zonal and monthly mean ozone columns and $\Delta EUV(j)$ contains the change in monthly effective UV resulting from a change of 1 DU in the ozone column. Thus, the effective UV for each geographical position can be obtained for January and July. Afterwards, the correction for the surface elevation can be applied to each location.

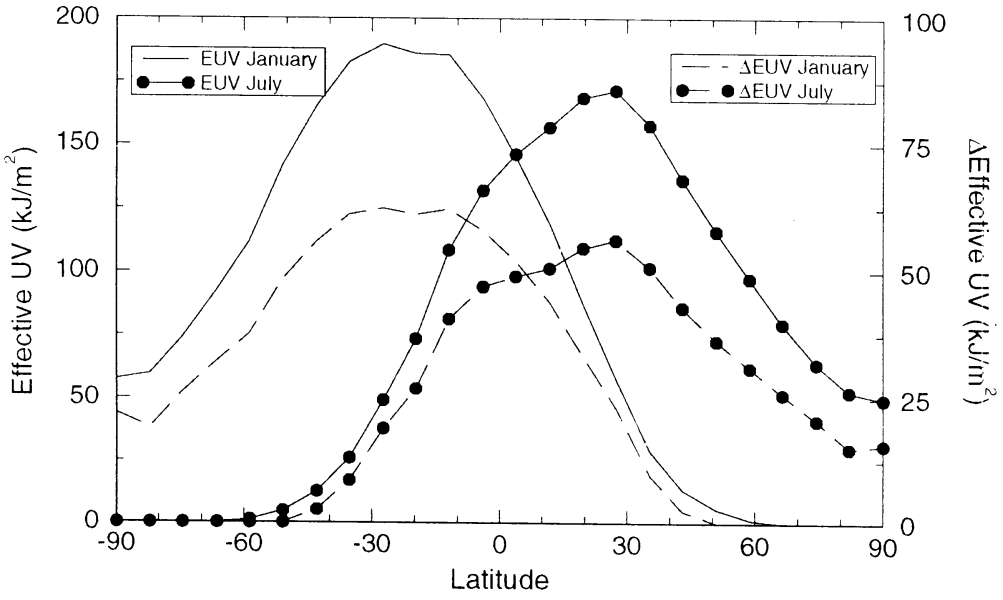

Figure 6. Calculated monthly effective UV (in kJ/m^2) and the change in monthly effective UV (in J/m^2) when increasing the ozone column 1 DU for each CTMK latitude for January and July.

The damaging effect of ultraviolet radiation on skin is generally an accumulating effect. Therefore the change in effective UV over the whole year is the quantity that should be considered. The monthly effective UV values show a large seasonal dependence. If January and July are considered, then the year amount of effective UV can be obtained by assuming a fixed ratio between the year effective UV value and the sum of the effective UV values in January and July. This ratio depends on latitude and is given in Fig. 7. The resulting change of effective UV in a year can be calculated by multiplying the sum of effective UV in January and July with this ratio. The use of this ratio gives better results than the assumption that the seasonal dependence of the monthly effective UV can be expressed as a sine.

As an illustration the change in effective UV due to the increase in ozone resulting from aircraft NO_x emissions (cf. Fig. 1) is given in Fig. 8 for July. The ozone increase leads to a decrease of the damaging UV at the surface and hence a decrease of effective UV. This decrease is shifted equatorward compared to the location of the largest ozone increase, because of the higher solar elevation. The decrease in effective UV is maximally about 1 percent over Siberia.

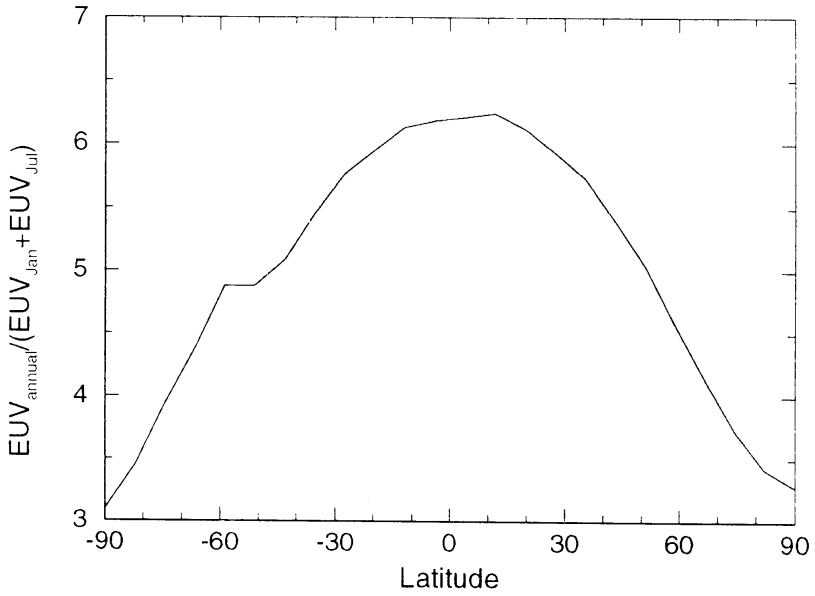

Figure 7. Ratio of the annual effective UV to the summed monthly effective UV for January and July as a function of latitude.

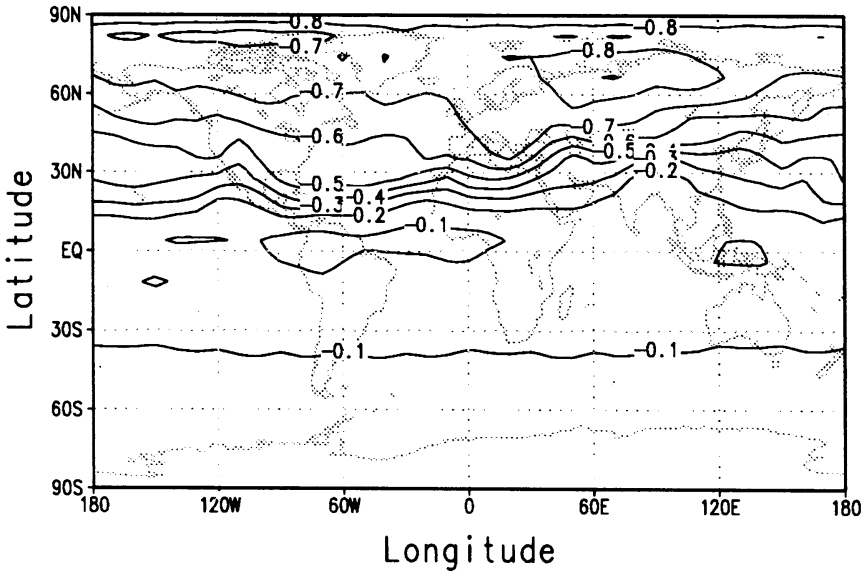

Figure 8. Relative change in effective UV (in %) due to ozone changes from aircraft NO_x emissions for July.

4. Outlook

In cooperation with IMAU and RIVM-LLO within the framework of the AIRFORCE (Aircraft Influences and Radiative Forcing from Emissions) project the CTMK model will be validated and extended to include the stratosphere. Further tests of the AERO modules will be performed in the beginning of 1997 when all required data are available. A detailed user document will be published in cooperation with Resource Analysis. The CTMK model will also be used in the forthcoming European assessment of the impact of subsonic aircraft emissions upon the atmospheric composition.

5. References

AERONOX, "The Impact of NO_x Emissions from Aircraft upon the Atmosphere at Flight Altitudes 8-15 km", U. Schumann (ed.), EC-DLR Publication on Research Related to Aeronautics and Environment, Brussels, 1995

K.L. Emmons, et al., "Climatologies of NO_x and NO_y: A comparison of data and models", *Atm. Env.*, in press, 1997

J.P.F. Fortuin, R. van Dorland, W.M.F. Wauben and H. Kelder: "Greenhouse effects of aircraft emissions as calculated by a radiative transfer model", *Ann. Geophysicae* **13**, 413-418, 1995

IPPC, "Climate Change 1994", J.T. Houghton *et al.* (Eds.), Cambridge University Press, Cambridge, 1995

F. Kuik and H. Kelder, "Spectral ultraviolet radiation measurements and correlation with atmospheric parameters", Scientific report, WR **94-05**, KNMI, De Bilt, The Netherlands, 1994

E. Matthews, "Global vegetation and land use: New high-resolution data bases for climate studies", *J. Clim. Appl. Meteor.* **22**, 474-487, 1983

J.W. Pulles, S. Lowe, R. van Drimmelen, G. Baarse and P. McMahon, "The AERO-project: model description and current status", Internal report, RLD, The Hague, The Netherlands, 1995

W.M.F. Wauben, P.F.J. van Velthoven and H. Kelder, "Chemistry and Transport of NO_x Aircraft Emissions in a Global 3-D Chemical Transport Model, in *International Scientific Colloquium on the Impact of Emissions from Aircraft and Spacecraft upon the Atmosphere*, U. Schumann and D. Wurzel (eds.), DLR Mitteilungen **94-06**, Cologne, 1994

W.M.F. Wauben, P.F.J. van Velthoven and H. Kelder, "Changes in tropospheric NO_x and O_3 due to subsonic aircraft emissions", Scientific report, WR **95-04**, KNMI, De Bilt, The Netherlands, 1995a

W.M.F. Wauben, J.P.F. Fortuin, P.F.J. van Velthoven and H. Kelder, "Interim report on the KNMI contributions to the second phase of the AERO-project", KNMI Technical report TR-**181**, De Bilt, The Netherlands, 1995b

W.M.F. Wauben, P.F.J. van Velthoven and H. Kelder, "A 3D chemistry transport model study of changes in atmospheric ozone due to aircraft NO_x emissions", *Atm. Env.*, in press, 1997a

W.M.F. Wauben, P.F.J. van Velthoven and H. Kelder, "The impact of air traffic in the NAFC during POLINAT: Model results and measurements", to appear in POLINAT final report, 1997b

W.M.F. Wauben, J.P.F. Fortuin and H. Kelder, "Sensitivity of radiative forcing due to changes in the global distribution of ozone with application to ozone changes from aviation", submitted to the Quadrennial Ozone Symposium, Aquila, Italy, 1997c

W.M.F. Wauben, J.P.F. Fortuin, P.F.J. van Velthoven and H. Kelder, "Validation of modelled ozone distributions with sonde and satellite observations", submitted to *J. Geophys. Res.*, 1997d